Strong Generation of Coherent Acoustic Phonons in Semiconductor Quantum Dots

A. Devos,[1,*] F. Poinsotte,[2] J. Groenen,[2,4] O. Dehaese,[3] N. Bertru,[3] and A. Ponchet[4]

[1]*Institut d'Électronique, de Microélectronique et de Nanotechnologie, UMR 8520, Avenue Poincaré, B.P. 69, F-59652 Villeneuve d'Ascq Cedex, France*

[2]*Laboratoire de Physique des Solides UMR 5477, IRSAMC, Université Paul Sabatier, 118 route de Narbonne, F-31062 Toulouse Cedex 4, France*

[3]*Institut National des Sciences Appliquées, 20 avenue des Buttes de Coesmes, F-35043 Rennes Cedex, France*

[4]*CEMES CNRS, B.P. 94347, 31055 Toulouse Cedex 4, France*

(Received 21 July 2006; published 17 May 2007)

We present experimental results obtained in two-color pump-probe experiments performed in semiconductor self-assembled quantum dot (QD) layers. The sample reflectivities present several acoustic contributions, among which are strong acoustic phonon wave packets. A comparison between one- and two-color experiments and a fine analysis of the echo shape attest that a high magnitude phonon pulse emerges from each single QD layer. This conclusion is supported by a numerical modeling which perfectly reproduces our experimental signals only if we introduce a strong generation in each QD layer. We explain such a strong emission thanks to an efficient capture of the carriers by the QDs.

DOI: 10.1103/PhysRevLett.98.207402 PACS numbers: 78.67.Hc, 43.35.+d, 78.20.Hp, 78.47.+p

The interaction between phonons and electrons is a crucial issue in nanophysics due to the role it plays in carrier relaxation [1–3]. This has motivated much work on the vibrational modes of nanocrystals and quantum dots (QDs) using resonant Raman scattering and ultrafast optical spectroscopy. Femtosecond laser pulses in a pump-probe scheme offer a unique way of directly observing phonons in the time domain [4]. Several mechanisms have been proposed for the excitation and the detection of phonons using ultrashort optical pulses: impulsive stimulated Raman scattering [5], thermal expansion in metallic nanostructures [6,7], deformation potential [8,9], and piezoelectric coupling [10].

Phonon studies by time-resolved pump-probe experiments can be listed in two categories. First, most of these experiments have been applied to the study of confined vibrational modes in both metallic and semiconducting nanostructures. The transient transmission or reflectivity reveals in the first tens of picoseconds an oscillating part which is assigned to vibrational normal modes of the nanostructure [5,6,10–12]. Such a regime is obtained in dots whose mechanical properties significantly differ from those of the matrix, vibrational modes being confined. Second, a few other time-resolved studies were reported on semiconductor heterostructures which present a small acoustic mismatch. These studies deal mainly with quantum wells, in which the light pulses excite and detect ballistic phonon wave packets whose propagation is monitored on a larger time scale [8,9,13]. Interaction between acoustic phonons and electrons in epitaxially grown semiconductor QD (i.e., self-assembled QDs) layers has been attracting much interest recently [1–3].

In this Letter, we report on time-resolved experiments on such semiconductor QD layers. We detected strong pulses in the reflectivity which are unquestionably assigned to coherent acoustic phonon wave packets emitted from each QD layer and detected at the sample surface. To the best of our knowledge, this is the first direct evidence of a strong coherent acoustic phonon emission from a QD layer. The most noticeable points are the high intensity of the detected phonon pulses and the large wavelength range on which the emission is found to be efficient. These results suggest that semiconductor QDs could be an efficient source of coherent acoustic phonons needed for nanoscale acoustic transduction.

Experiments were carried out on samples grown by gas source molecular beam epitaxy on (100) InP substrates as described elsewhere [14]. We present here the results obtained on two samples hereafter designated by *A* and *B* containing, respectively, two and one layers of buried InAs/InP QDs. In sample *A*, the nominal thicknesses of the final cap and the interlayer are, respectively, 320 and 480 nm. In sample *B*, the nominal cap thickness is 400 nm. Transmission electron microscopy observations have shown islands of quantum size, with an average height of 2 nm and an average width of 20 nm. The time-resolved experiments were conducted using a two-color pump and probe setup associated with a tunable Ti:sapphire oscillator. The laser produces 120 fs optical pulses at a repetition rate of 76 MHz centered at a wavelength adjustable between 700 and 990 nm. Figure 1(a) presents a schematic diagram of the experimental setup. The pump pulse is directly issued from the infrared oscillator, whereas the probe is frequency doubled to produce a blue pulse which is absorbed near the sample surface in the InP cap. All of the experiments are performed at room temperature.

Figure 1(b) shows the transient reflectivity of sample *A* obtained using a 812 nm pump and a blue probe which detects only the reflectivity changes at the sample surface. The photogenerated carriers first produce an initial spike visible on the ultrafast time scale ($\leq$1 ps). The subsequent long-lived change in reflectivity is caused by thermally and

electronically induced variations in the cap layer refractive index. The reflectivity also presents strong localized structures (at $T_1 = 70$ ps and $T_2 = 175$ ps) to which this Letter is devoted. As we demonstrate in the following, they correspond to acoustic phonon wave packets generated in each QD layer.

To go further, we present in Fig. 2(a) the experimental signals obtained on samples A and B after substracting a fit of the relaxation contribution. One first notes that in both samples the number of strong detected structures (in the following designated by ''echo'') is equal to the QD layer number (two for sample A at T_1 and T_2 and one for sample B at T_1'). The echo delays correspond to the time needed for a longitudinal acoustic wave to go from the QD layers to the surface.

The substraction of the relaxation contribution also reveals several smaller acoustic signals. In the first picoseconds, the response of both samples displays a small oscillating part. It originates from the detection of the acoustic pulse generated at the free surface and which propagates towards the substrate. The blue pulses probe only a few tens of nanometers in the InP cap (the absorption length in InP close to 20 nm at 400 nm is much shorter than the cap thickness in both samples). The oscillating character is related to the photoelastic detection mechanism [15]. To confirm this point, we measured the oscillation period (T) as a function of the probe wavelength (λ_{probe}) [Fig. 2(b)]. It reveals a very good agreement with the theoretical result expected from a photoelastic model: $T = \lambda_{\text{probe}}/2n\upsilon$, where the optical index (n) and the longitudinal sound velocity (υ) were extracted from the literature [16].

A small part of this acoustic pulse is reflected on the first QD layer, which leads to a small structure detected at a delay which corresponds to a round-trip in the InP cap. In sample A (respectively, B), such a structure is detected at $2T_1 = 140$ ps (respectively, $2T_1' = 176$ ps). These delays correspond to those expected after one round-trip in 321 nm of InP (respectively, 403 nm); both values are very close to the nominal cap thicknesses (320 and 400 nm, respectively).

In Fig. 2(a), we also present the experimental result obtained using a blue beam for both the pump and the probe on sample A. Compared to the previous results, only the generation is thus expected to be modified due to the strong optical absorption of the pump pulse in the final cap. The small echo corresponding to the round-trip in the cap is still detected. That is consistent with the fact that this echo results from a generation and a detection near the free surface. The most noticeable point in the comparison between two-color and one-color experiments is the extinction of the strong acoustic structures detected at T_1 and T_2. Because of the wavelength change, no blue pump light can reach the QD layers. This observation thus confirms that the strong coherent acoustic phonon wave packets are issued from the QD layers.

This conclusion is also supported by a fine comparison of the shape of the successive localized acoustic signals. The strong echo detected at T_1, the small structure at $2T_1$ (round-trip in the cap), and a small echo close to $3T_1 = 210$ ps correspond to the detection of the acoustic energy coming from the first QDs layer and reflected by the free surface back into the sample and then reflected by this QD layer back to the surface. These signals have been rescaled and temporally superimposed in Fig. 2(c). The figure reveals that the structures detected at T_1 and $3T_1$ present the same shape. On the contrary, the echo detected at $2T_1$ differs from the others, its shape being much symmetrical

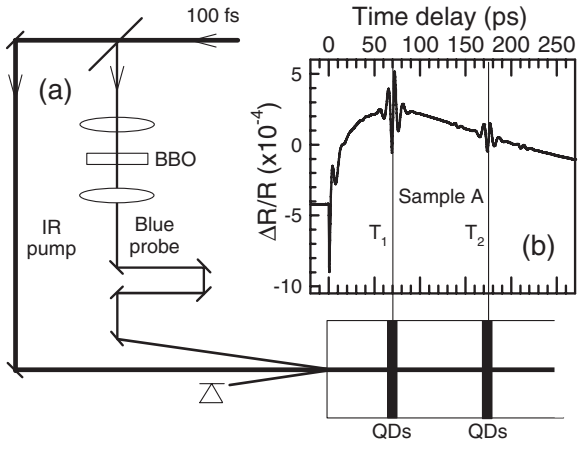

FIG. 1. (a) Schematic diagram of the experimental setup. Most experiments were carried out using an infrared pump and a blue probe. BBO = β-BaB_2O_4 crystal. The infrared pump significantly penetrates the sample, whereas the blue pulses only probe the sample surface. (b) Experimental result obtained using a two-color experiment with pulses centered at 812 nm on a two-QD layer sample. The most noticeable point is the structures localized at $T_1 = 70$ and $T_2 = 175$ ps.

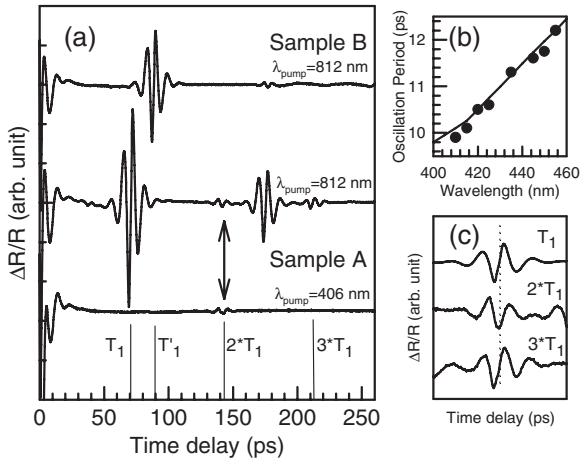

FIG. 2. (a) Experimental results obtained on samples A and B containing two and one QD layers, respectively, using various pump and probe colors. (b) Period of the oscillation detected at zero delay as a function of the probe wavelength. (c) Shape comparison between the three first acoustic echoes. One should note that the structures detected at T_1 and 3^*T_1 can be perfectly superimposed contrary to the 2^*T_1 one.

than theirs. As in the three cases where the detection acts at the surface, the observed difference is thus related to the strain pulse itself. A pulse generated at the free surface has a bipolar shape due to boundary conditions, whereas the strain pulse generated inside the sample is expected to be monopolar. The photoelastic detection of a bipolar (respectively, monopolar) strain leads to a symmetrical (respectively, asymmetrical) echo. The asymmetrical shape of the T_1 and $3T_1$ echoes is one more evidence of an acoustic emission from the QD layer.

From all of these results, we can thus conclude that coherent acoustic phonons are generated from the sample surface and from each QD layer. Using a numerical modeling of the generation and detection processes, we can examine independently the acoustic generation from the successive layers of the sample. The numerical tool first solves the electromagnetic continuity equations in order to get the pump absorption profile in the sample which serves as a source term in the resolution of the acoustic continuity equations. The first derivation of the model can be found in Ref. [17]. The input parameters are the optical and mechanical parameters of materials, an effective generation parameter, and a complex photoelastic constant for the detection.

Figure 3 presents numerical and experimental results obtained on sample *A*. We first consider the generation acting only in InP layers. By fitting the photoelastic constants, we can well reproduce the intensity and phase of the experimental oscillation detected in the first picoseconds [Figs. 3(a) and 3(c)]. The 810 nm pump can reach up to 1 μm in the sample depth. Even in the case of a generation limited to InP, each QD layer introduces a discontinuity in the absorption and generation profiles. The resulting strain pulse also presents such discontinuities, and its photoelastic detection gives echoes at T_1 and T_2 as shown in Fig. 3(c). Nevertheless, these structures cannot correspond to the measured echoes for two obvious reasons revealed in the comparison of Figs. 3(a) and 3(c). First, the phase of the numerical structures is opposite to the experimental one. Second, in this scheme, the numerical echoes cannot be higher than the first picoseconds oscillation due to the absorption profile that is unlike the experimental observation. To reach the excellent agreement between theory and experiment presented in Figs. 3(a) and 3(b), we need to introduce a strong generation from the InAs QDs. The numerical study further demonstrates the strong acoustic generation in the self-assembled InAs/InP QD layers.

We now focus on the spectroscopic behavior of the phenomenon. Figure 4 shows the first 100 ps of experimental and numerical signals obtained in sample *A* using a two-color setup at different laser wavelengths comprised between 750 and 900 nm. One first notices that strong echoes are still detected over this large wavelength range. This result contrasts with the sharp resonance previously reported in quantum wells [9]. The only significant change concerns the echo shape. We reported similar effects on metals and semiconductors [18–20]. Here the InP E_1

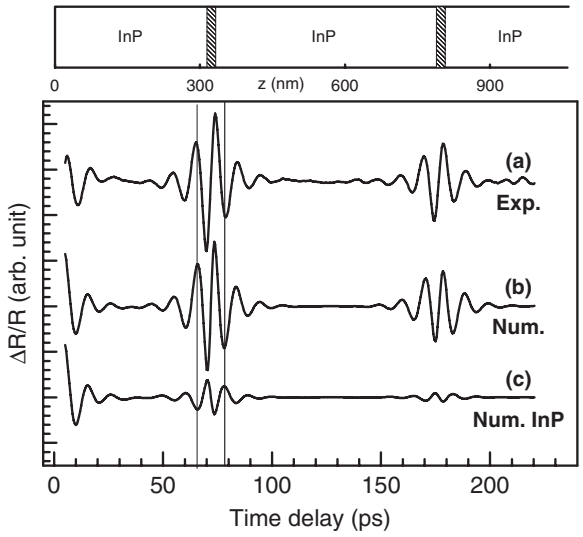

FIG. 3. (a) Experimental result obtained on sample *A* after substracting of the relaxation contribution. (b) Complete numerical result. (c) Numerical modeling of the acoustic contributions issued from the InP layers of the sample. The excellent agreement obtained between (a) and (b) requires a high generation process in the QD layer.

transitions (394 nm [16]) fall in the blue probe wavelength range (375–450 nm). In the vicinity of an interband electronic transition, changes in the photoelastic couplings occur and affect the detected echo shape and/or amplitude. By fitting the photoelastic coefficients, we obtained a perfect agreement between experiment and simulation for each wavelength, using literature values for the index of refraction [21,22]. To fit the echo shape, a phase change in the photoelastic constant is sufficient. We emphasize that a large generation coefficient in QDs is still needed to reproduce each echo amplitude. This demonstrates that the detection mechanism is well accounted for and that the phonon emission is strong over the whole wavelength range.

Different mechanisms can play a role in the acoustic phonon emission from a light pulse in semiconductors [23]. But the deformation-potential (DP) mechanism is expected to have the strongest contribution here. Indeed, the thermoelastic mechanism, which is based on a sudden change in the lattice temperature, cannot reproduce such a high generation assuming realistic values for optical absorption and dilatation in the InAs QD layer. The piezoelectric mechanism is not relevant here due to the (100) orientation. For the DP mechanism, an acoustic pulse results from the change in the electronic state occupation, and it is governed by the product of the carrier density by the deformation potential itself. Nevertheless, the echo amplitudes one calculates, by assuming that the photoexcited carrier density in the QD layer is given by light absorption, are much lower than those observed experimentally. The high amplitude of the phonon wave packet generation can be accounted for by considering the follow-

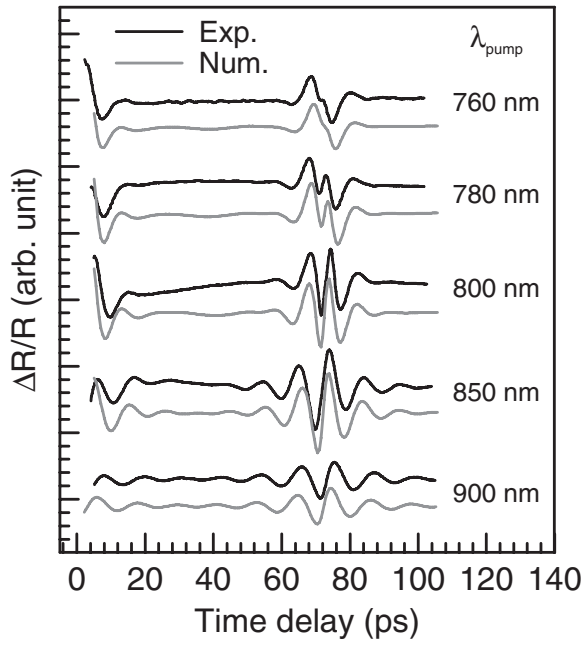

FIG. 4. Experimental results obtained on sample *A* at different laser wavelengths using a two-color pump-probe setup. For each wavelength, we also present a numerical fit.

ing scenario, in which the QD layers play a specific role. Because of the high energy of the pump pulse compared to the QD states, electron-hole pairs are generated mainly in the barrier continuum states. In a very short time (≤ 1 ps), the carriers lose their energy and are captured by the QDs where a high carrier density results [24]. The carrier density which acts in the deformation-potential mechanism is thus much higher than expected solely from direct light absorption. The carrier capture explains the high observed emission. It also accounts for the nonresonant character of the generation since the barrier states present a large absorption band. Within this scenario, generation can be expected even when light does not reach the QD layer provided the carrier capture can act. It is worth mentioning that an efficient phonon emission has been observed in a sample with a 120 nm cap layer pumping at 400 nm, a wavelength at which light is strongly absorbed within 18 nm InP. For samples with a much thicker cap, the generation does not operate anymore (as shown in Fig. 2, sample *A* has a 320 nm thick cap layer).

This is the first direct observation of a phonon emission from self-assembled QDs. It is found to be independent on the substrate orientation [we obtained similar results on samples grown on (311) and (100) substrates] and does not require any particular in-plane QD arrangement. These results contrast with a recent observation of oscillations in the reflectivity on self-assembled QDs [25]. The authors observed a long-lived oscillation only for a specific in-plane distribution of QDs grown on a (311) substrate. They proposed an interpretation in terms of a phonon emission invoking the piezoelectric coupling due to the (311) substrate orientation.

We have reported on strong acoustic phonon wave packets emission from a QD single layer. The most noticeable points are the high magnitude of the detected signal and its nonresonant character. We explain the high phonon emission by involving an efficient carrier capture. That suggests that QD layers could be promising systems for a very efficient generation of phonon pulses whose applications in phonon physics is strongly needed. The strong localization of the emission demonstrated here suggests that a QD layer should also act as a particularly high frequency acoustic emitter.

*Electronic address: Arnaud.Devos@isen.fr

[1] C. Kammerer *et al.*, Phys. Rev. B **65**, 033313 (2001).
[2] E. A. Muljarov *et al.*, Phys. Rev. Lett. **93**, 237401 (2004).
[3] A. Krugel *et al.*, Phys. Rev. B **73**, 035302 (2006), and references therein.
[4] R. Merlin, Solid State Commun. **102**, 207 (1997).
[5] A. V. Bragas *et al.*, Phys. Rev. B **69**, 205306 (2004).
[6] M. Nisoli *et al.*, Phys. Rev. B **55**, R13 424 (1997).
[7] J. H. Hodak *et al.*, J. Chem. Phys. **108**, 9210 (1998).
[8] J. J. Baumberg *et al.*, Phys. Rev. Lett. **78**, 3358 (1997).
[9] O. Matsuda *et al.*, Phys. Rev. B **71**, 115330 (2005).
[10] U. Ozgur *et al.*, Phys. Rev. Lett. **86**, 5604 (2001).
[11] T. Krauss and F. Wise, Phys. Rev. Lett. **79**, 5102 (1997).
[12] A. V. Bragas *et al.*, Phys. Rev. B **73**, 125305 (2006).
[13] R. Liu *et al.*, Phys. Rev. B **72**, 195335 (2005).
[14] C. Paranthoen *et al.*, Appl. Phys. Lett. **78**, 1751 (2001).
[15] C. Thomsen *et al.*, Opt. Commun. **60**, 55 (1986).
[16] O. Madelung, *Semiconductors Group IV Elements and III-V Compounds* (Springer-Verlag, Berlin, 1991).
[17] C. Thomsen *et al.*, Phys. Rev. B **34**, 4129 (1986).
[18] A. Devos *et al.*, Phys. Rev. Lett. **86**, 2669 (2001).
[19] A. Devos *et al.*, Phys. Rev. B **68**, 045405 (2003).
[20] A. Devos and R. Côte, Phys. Rev. B **70**, 125208 (2004).
[21] D. E. Aspnes *et al.*, Phys. Rev. B **27**, 985 (1983).
[22] S. Adachi, Phys. Rev. B **35**, 7454 (1987).
[23] V. E. Gusev and A. A. Karabutov, *Laser Optoacoustics* (Institute of Physics, Woodbury, NY, 1993).
[24] S. Hinooda *et al.*, Appl. Phys. Lett. **78**, 3052 (2001).
[25] E. W. Bogaart *et al.*, Appl. Phys. Lett. **88**, 143120 (2006).